# Enhanced electromechanical coupling in SAW resonators based on sputtered non-polar $Al_{0.77}Sc_{0.23}N$ $(11\bar{2}0)$ thin films

Cite as: Appl. Phys. Lett. **116**, 101903 (2020); https://doi.org/10.1063/1.5129329
Submitted: 29 September 2019 • Accepted: 21 February 2020 • Published Online: 12 March 2020

Anli Ding, Lutz Kirste, Yuan Lu, et al.



Applied Physics Letters ARTICLE scitation.org/journal/apl

# Enhanced electromechanical coupling in SAW resonators based on sputtered non-polar $Al_{0.77}Sc_{0.23}N$ $(11\bar{2}0)$ thin films

Cite as: Appl. Phys. Lett. **116**, 101903 (2020); doi: 10.1063/1.5129329
Submitted: 29 September 2019 · Accepted: 21 February 2020 ·
Published Online: 12 March 2020



Anli Ding,[1,a)] Lutz Kirste,[1] Yuan Lu,[1,b)] Rachid Driad,[1] Nicolas Kurz,[2] Vadim Lebedev,[1] Tim Christoph,[1] Niclas M. Feil,[2] Roger Lozar,[1] Thomas Metzger,[3] Oliver Ambacher,[1,2] and Agnė Žukauskaitė[1]

## AFFILIATIONS

[1]Fraunhofer Institute for Applied Solid State Physics IAF, Tullastrasse 72, 79108 Freiburg, Germany
[2]Department of Sustainable Systems Engineering, University of Freiburg, Emmy-Noether-Strasse 2, 79110 Freiburg, Germany
[3]Qualcomm Germany RFFE GmbH, Anzinger Strasse 13, 81671 Munich, Germany

[a)]Author to whom correspondence should be addressed: anli.ding@iaf.fraunhofer.de
[b)]**Present address:** Evatec China Ltd 2002A, Tower B, Dawning Center, Hongbaoshi Road 500, 201103 Shanghai, People's Republic of China.

## ABSTRACT

Non-polar a-plane $Al_{0.77}Sc_{0.23}N$ $(11\bar{2}0)$ thin films were prepared by magnetron sputter epitaxy on r-plane $Al_2O_3(1\bar{1}02)$ substrates. Different substrate off-cut angles were compared, and the off-cut angle of 3° resulted in the best structural quality of the AlScN layer. Structural characterization by x-ray diffraction confirmed that single phase, wurtzite-type, a-plane AlScN $(11\bar{2}0)$, surface acoustic wave resonators were fabricated with wavelengths $\lambda = 2$–$10\,\mu$m (central frequency up to 1.7 GHz) with two orthogonal in-plane propagation directions. A strong dependence of electromechanical coupling on the in-plane orientation was observed. Compared to conventional c-plane AlScN based resonators, an increase of 185–1000% in the effective electromechanical coupling was achieved with only a fractional decrease of $<10.5\%$ in series resonance frequency.



Due to the enhanced piezoelectric coefficient[1] and significantly improved electromechanical coupling,[2] AlScN is currently being considered as an attractive alternative to AlN thin films and $LiNbO_3$ bulk crystals in RF filter components, which are needed in next generation high-frequency high-bandwidth mobile communication applications. Because of CMOS compatibility of such substrates such as silicon Si(001), it is more often chosen for Al(Sc)N growth. However, only c-axis oriented nitride layers can be grown on Si(001), which led to mostly c-plane AlScN(0001) being investigated for the fabrication of various electroacoustic resonators for RF filters, such as surface acoustic waves (SAWs),[3–5] bulk acoustic waves (BAWs),[6,7] or Lamb wave resonators (LWRs).[8–10] One of the main obstacles in utilizing $Al_{1-x}Sc_xN$-based electroacoustic devices to their full potential remains the metastability of the material. It can lead to crystal lattice distortion, misoriented grains,[11] elemental segregation, or even phase separation into wurtzite AlN, and rock salt ScN when the Sc concentration approaches $x = 0.5$,[12] thus hindering the device fabrication and having a negative impact on the device performance. Conversely, several recent reports suggest that even with conventional materials, e.g., AlN, GaN, or ZnO, further improvement in the electromechanical coupling of SAW resonators is possible by changing from polar c-plane to non-polar a-plane oriented layers to promote the propagation of acoustic waves.[13,14] Consequently, by combining both, a material with higher electromechanical coupling like AlScN and switching from the c-plane to the a-plane orientation of the thin film, one could expect even higher benefit in the final device performance while keeping the Sc concentration relatively low. Furthermore, a-plane AlScN-based SAW resonators were theoretically investigated,[15–18] and indeed, studies predicted the improved coupling of a-plane resonators compared to those based on the c-plane material.[15,16]

Several attempts have been made to influence the c-axis angle of the AlScN thin films mostly deposited on Al/silica glass.[19–24] However, the c-axis tilt angle of $Al_{1-x}Sc_xN$ was at maximum 80° with the Sc concentration $x$ not higher than only 0.05, and no electromechanical coupling or quality factor values were reported.[23] Furthermore, the experimental growth of AlScN on $Al_2O_3(1\bar{1}02)$ has been mentioned in only two studies.[15,25] In the first,[15] a c-axis tilt angle of 33.1° or less was obtained, whereas in the second,[25] the growth parameters were not optimized, resulting in polycrystalline films.

In this work, the magnetron sputter epitaxy (MSE) process was used to grow single phase, non-polar, a-plane $Al_{0.77}Sc_{0.23}N$ $(11\bar{2}0)$/$Al_2O_3(1\bar{1}02)$ thin films, and SAW resonators were fabricated with central frequencies up to 1.7 GHz. We show the significantly improved electromechanical coupling and figure of merit (FOM) of a-plane $Al_{0.77}Sc_{0.23}N$-based SAW resonators with respect to c-plane $Al_{0.77}Sc_{0.23}N$-based resonators and only a slight decrease in the resonant frequency.

1 $\mu$m a-plane $Al_{0.77}Sc_{0.23}N$ $(11\bar{2}0)/Al_2O_3(1\bar{1}02)$ and c-plane $Al_{0.77}Sc_{0.23}N(0001)/Al_2O_3(0001)$ thin films were prepared by reactive pulsed-DC magnetron sputtering using 99.99% pure Sc and 99.9995% pure Al sputter targets at heater temperatures up to 500 °C. 20 sccm nitrogen ($N_2$) flow was used as the process gas, and the combined magnetron power $P(\text{Al}) + P(\text{Sc})$ of 1000 W was used to produce layers with the composition of $Al_{0.77}Sc_{0.23}N$. The base pressure before the growth was $<5 \times 10^{-6}$ Pa. More details about the optimization of the growth parameters can be found elsewhere.[26,27] The Sc content, expressed as Sc/(Al+Sc), was determined using SIMS and energy dispersive x ray (EDX) in AlScN(0001)/Si(001) layers deposited under the same conditions in order to avoid the overlap of the Al signal from the film and the substrate.[26] X-ray diffraction (XRD) $2\theta/\theta$ scans and $Al_{1-x}Sc_xN$ $11\bar{2}0$ reflection rocking curve ($\omega$-scan) measurements, as well as pole figure measurements, were performed to evaluate the orientation and the crystalline quality of the films using a PANalytical X'Pert Pro MRD diffractometer with a Ge 220 hybrid monochromator providing Cu-K$\alpha_1$ radiation.

In order to evaluate the potential of a-plane and c-plane $Al_{0.77}Sc_{0.23}N$ thin films for implementation in RF-MEMS, SAW resonators were fabricated. Electron beam (e-beam) evaporation together with stepper photolithography/lift-off processes was employed to transfer 100 nm thick platinum (Pt) patterns of the interdigital transmission (IDT) and the reflectors onto the thin films. The IDTs consisted of 100 fingers, while each reflector bank had 40 short-circuited fingers; their pitch $p = \lambda/2$ was varied for fabricating resonators with the wavelengths $\lambda$ of 2, 2.5, 3, 4, 5, 6, 7, 8, and 10 $\mu$m. a-plane $Al_{0.77}Sc_{0.23}N$-based resonators were fabricated with two orthogonal in-plane propagation directions, i.e., parallel and perpendicular to the primary flat of the substrate (in the following referred to as "0°" and "90°" resonators, respectively). For contact pads, a 20/100 nm thick titanium/gold (Ti/Au) stack was evaporated using the same techniques. The fabricated resonators were analyzed by measuring their frequency response at the wafer level by using an Agilent E5061B vector network analyzer (VNA) and cascade air coplanar SG probes (350 $\mu$m pitch). An impedance standard substrate (ISS) from Cascade Microtech was used for calibration in the open-short-load configuration before performing the measurements.

Non-polar group III-nitride layers have various applications, but until now, most groups focused on using different types of metalorganic chemical vapor deposition (MOCVD) and MBE approaches for growth. In previous studies of sputtered a-plane AlN, it was typically done in combination with ZnO acting as a buffer layer.[28] Based on the literature, the off-cut angle for r-plane $Al_2O_3$ $(1\bar{1}02)$ can have a significant influence on material quality and on the formation of in-plane anti-phase domains.[29] The control of anti-phase domains is especially important in electroacoustic applications as different directions of the c-axis would impede the propagation of acoustic waves and have a negative impact on electromechanical coupling. Wu *et al.*[29] also showed that a "positive" substrate off-cut angle in the direction of the c-plane facilitates the growth of a better oriented a-plane AlN. However, in the literature, the actual off-cut angle that is the most suitable to produce high quality material varies. In addition, in the case of AlScN, the lattice parameters are slightly larger than those of AlN, so the lattice mismatch is also different. Therefore, we performed growth experiments on three kinds of r-plane $Al_2O_3$ substrates with 1°, 2°, and 3° off-cut angles toward the c-plane before proceeding with device fabrication.

The results of XRD $2\theta/\theta$ measurements are shown in Fig. 1. In addition to $Al_2O_3$ $1\bar{1}02$ type peaks originating from the substrate, only the $Al_{0.77}Sc_{0.23}N$ $11\bar{2}0$ diffraction peak can be seen in all three cases, indicating the growth of the single-phase a-plane oriented $Al_{0.77}Sc_{0.23}N$ thin films. The rocking curve measurements (inset in Fig. 1) show a much stronger reflection in the case of 3° off-cut, and the full width at half maximum (FWHM) of this peak decreases from 2.25° in the case of 1° off-cut down to 1.72° for 3° off-cut. Such rocking curve FWHM values are comparable to our $AlScN(0001)/Al_2O_3(0001)$ data previously published in Ref. 27, indicating sufficient material quality for the fabrication of high frequency SAW resonators. Additionally, pole figure measurements (not shown) were performed, and they indicate that the films were deposited with a defined in-plane orientation, confirming the good application of the MSE growth method for also non-polar AlScN thin films. However, the non-polar AlScN layers show a complex distortion from the exact hexagonal symmetry due to the lattice mismatch and the off-cut angle of the substrate. Details of this distortion and the epitaxial relationship are not the subject of this work and will be published elsewhere.

Based on VNA and laser Doppler vibrometer (LDV) measurements, SAWs were excited in all the fabricated resonators. Series and parallel resonance frequencies $f_s$ and $f_p$, respectively, were extracted using the modified Butterworth van Dyke model (mBVD),[30] as described in more detail elsewhere.[12,31] The measured and fitted frequency response of the c-plane and a-plane based $\lambda = 2$ $\mu$m resonators

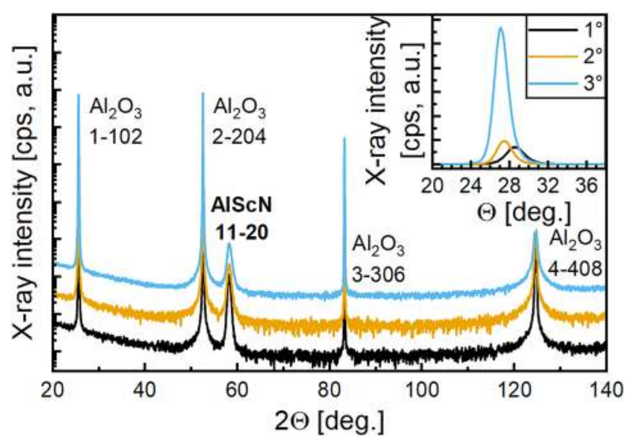


**FIG. 1.** X-ray diffraction $2\theta/\theta$ scans for sputter-deposited $Al_{0.77}Sc_{0.23}N$ $(11\bar{2}0)$/$Al_2O_3(1\bar{1}02)$ thin films with different substrate off-cut angles: 1° (black), 2° (orange), and 3° (blue). The inset shows the $\omega$-rocking curve for the $Al_{0.77}Sc_{0.23}N$ $11\bar{2}0$ peak.

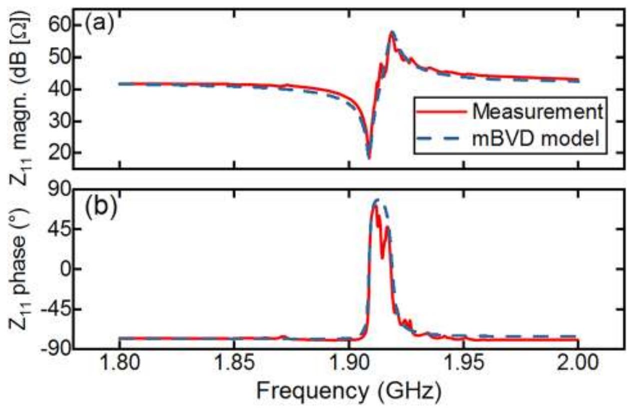


**FIG. 2.** Measured and fitted frequency response of c-plane $\lambda = 2\,\mu$m resonators according to the modified Butterworth van Dyke model: (a) impedance magnitude and (b) impedance phase.

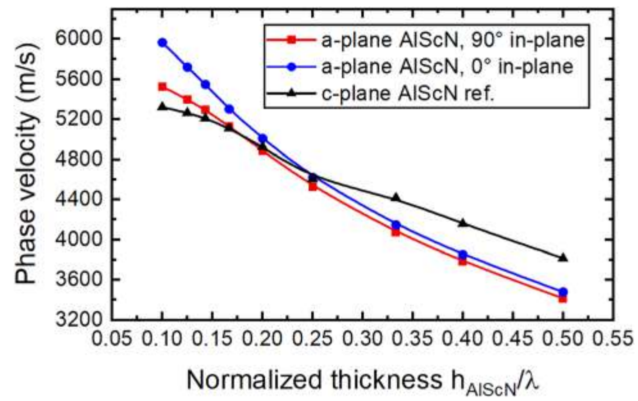


**FIG. 4.** Phase velocity dispersion curves of $Al_{0.77}Sc_{0.23}N$ $(11\bar{2}0)/Al_2O_3(1\bar{1}02)$ SAW resonators oriented parallel (blue circles) and perpendicular (red squares) to the primary substrate flat and reference $Al_{0.77}Sc_{0.23}N(0001)/Al_2O_3(0001)$ SAW resonators (black triangles). The lines are a guide to the eye.

is shown in Figs. 2 and 3, respectively. Satellite resonances can be seen in the former, the reason for which is not clear. Phase velocity $\nu_{ph}$ was then estimated from $f_s$ using

$$\nu_{ph} = \lambda f_s. \quad (1)$$

The resulting $\nu_{ph}$ dispersion curves are shown in Fig. 4 and Table I summarizes the performance of $\lambda = 2\,\mu$m resonators. When the normalized thickness $h_{AlScN}/\lambda$ is $<0.2$, the phase velocity and, by extension, resonant frequency $f_s$ are higher in the resonators fabricated on $Al_{0.77}Sc_{0.23}N$ $(11\bar{2}0)/Al_2O_3(1\bar{1}02)$. Specifically, at $h_{AlScN}/\lambda = 0.1°$, 90°, and 0°, a-plane resonators exhibit 3.9% and 12.1% higher $\nu_{ph}$ than c-plane resonators. At higher normalized thicknesses, i.e., $0.33 \leq h_{AlScN}/\lambda \leq 0.5$, the phase velocity and frequency of a-plane resonators are reduced, but the difference between the two investigated propagation directions in a-plane $Al_{0.77}Sc_{0.23}N$ is much smaller. At the other extreme, i.e., $h_{AlScN}/\lambda = 0.5$, the $\nu_{ph}$ of 90° and 0° a-plane resonators is 10.5% and 8.9% below those of c-plane resonators. At low normalized thickness $h_{AlScN}/\lambda$, SAW energy penetrates deeper into the substrate and is more affected by the anisotropic elastic properties of $Al_2O_3$. With increasing $h_{AlScN}/\lambda$, the substrate influence diminishes, and the intrinsic $\nu_{ph}$ of the piezoelectric layer becomes more important. At the same time, the anisotropic elastic properties of r-plane $Al_2O_3$ at least for the two propagation directions are much more pronounced than those of a-plane $Al_{0.77}Sc_{0.23}N$. Therefore, in terms of $\nu_{ph}$ and $f_s$, for the high frequency devices (i.e., high $h_{AlScN}/\lambda$), only a minuscule difference exists between the two investigated propagation directions on a-plane $Al_{0.77}Sc_{0.23}N$ and only a small difference when comparing both to the c-plane $Al_{0.77}Sc_{0.23}N$ resonators. The low standard deviations of frequency at a wafer level show good reproducibility and confirm uniform AlScN material quality across the wafer (Table I).

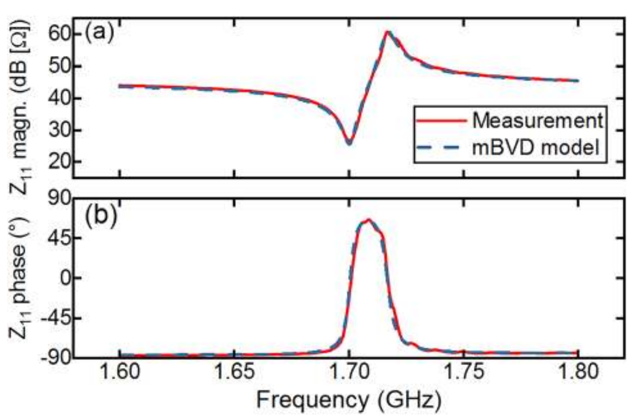


**FIG. 3.** Measured and fitted frequency response of a-plane 90° orientation $\lambda = 2\,\mu$m resonators according to the modified Butterworth van Dyke model: (a) impedance magnitude and (b) impedance phase.

The effective electromechanical coupling $k^2_{eff}$ was then calculated using the following equation:[32,33]

$$k^2_{eff} = \left(\frac{\pi}{2}\right)^2 \frac{f_s}{f_p}\frac{f_p - f_s}{f_p}. \quad (2)$$

Figure 5 shows $k^2_{eff}$ as a function of normalized thickness for all of the fabricated resonators. For conventional c-plane AlScN-based resonators, a relatively high effective electromechanical coupling $k^2_{eff}$[3,34] of 1.3% for the highest frequency resonators ($\lambda = 2\,\mu$m) was observed (black triangles). As it can be seen, the $k^2_{eff}$ of a-plane resonators parallel to the primary substrate flat (i.e., 0° rotated, blue circles) is lower than that of c-plane resonators. However, the $k^2_{eff}$ of 90° rotated resonators (red squares) is 350–1275% higher (depending on normalized thickness) and also 185–1000% higher compared to c-plane resonators with the same $h_{AlScN}/\lambda$. The results of our recently published FEM simulations,[16] which showed higher coupling of a-plane resonators compared to c-plane resonators, also confirm these observations. This enormous surge in electromechanical coupling with only a fractional decrease in the central frequency of SAW resonators would allow us to keep the Sc concentrations at a relatively low level where the losses caused by material imperfections are still moderate. Furthermore, such a strong dependence of electromechanical coupling in the in-plane orientation of the resonators could signal a possibility for further improvement if the resonators are aligned in-plane along other specific directions of the substrate, and a more detailed study of

**TABLE I.** Resonance frequency, effective electromechanical coupling, quality factor, and figure of merit (FOM) comparison for $\lambda = 2\,\mu$m resonators fabricated on c- and a-plane $Al_{0.77}Sc_{0.23}N$ grown on c- and r-plane $Al_2O_3$ substrates, respectively.

| For $\lambda = 2\,\mu$m | $f_s$ (GHz) | Relative change in $f_s$ | $k^2_{eff}$ (%) | Relative change in $k^2_{eff}$ | Quality factor, $Q_{s0}$ | FOM, $k^2_{eff} \cdot Q_{s0}$ |
|---|---|---|---|---|---|---|
| c-plane | $1.91 \pm 0.0063$ | | $1.3 \pm 0.2$ | | 659 | 8.6 |
| a-plane, 0° | $1.74 \pm 0.0045$ | −8.9 % | $0.5 \pm 0.03$ | −61.5 % | 321 | 1.6 |
| a-plane, 90° | $1.71 \pm 0.0086$ | −10.5 % | $2.4 \pm 0.1$ | +85 % | 538 | 12.9 |

the angular dependence for SAW performance will be published elsewhere.

The loaded series quality factor was calculated from mBVD model parameters using the following equation:[10,30]

$$Q_{s0} = \frac{1}{2\pi f_s (R_m + R_s) C_m}, \quad (3)$$

where $R_m$ and $R_s$ are the motional and series resistances, respectively, and $C_m$ is the motional capacitance. From the obtained values given in Table I, it can be seen that although the quality factor decreased by 18.4% for a-plane based resonators (90°), due to the mentioned 85% increase in electromechanical coupling, the figure of merit (FOM) is 50% higher.

In summary, single phase 1000 nm thick $Al_{0.77}Sc_{0.23}N$ c-plane and a-plane oriented thin films were sputter-deposited on c-plane and 1°–3° off-cut r-plane $Al_2O_3$ substrates, respectively. $Al_{0.77}Sc_{0.23}N$ $(11\bar{2}0)/Al_2O_3(1\bar{1}02)$-based SAW resonators were fabricated with $\lambda = 2$–$10\,\mu$m with two orthogonal in-plane propagation directions with respect to the primary flat of the substrate (0° and 90° rotated), and their performance was compared to $Al_{0.77}Sc_{0.23}N(0001)/Al_2O_3(0001)$-based resonators of the same design. In the case of 90° rotated a-plane resonators with the $\lambda = 2\,\mu$m wavelength, almost a twofold increase in the effective electromechanical coupling from $k^2_{eff} = 1.3\%$ to $k^2_{eff} = 2.4\%$ as compared to conventional c-plane AlScN-based resonators was observed. Despite the slight decrease in the quality factor, this led to a 50% increase in FOM. The highest value of $k^2_{eff} = 3.3\%$ was reached at $\lambda = 3\,\mu$m. Moreover, $\lambda = 2\,\mu$m 90° rotated resonators showed only a fractional decrease in a series resonance frequency of 10.5%. Interestingly, SAW resonator analysis indicated a very strong directional dependence and high potential for the additional improvement of device performance, which merits further investigations. This means that challenges caused by Sc incorporation into AlN could ultimately be overcome by focusing on non-polar and semi-polar AlScN thin films, taking us one step closer to the next generation mobile communication systems.

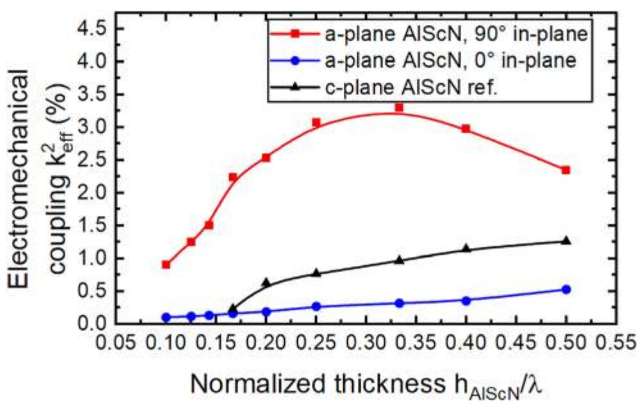


**FIG. 5.** Dispersion curves for the effective electromechanical coupling of $Al_{0.77}Sc_{0.23}N$ $(11\bar{2}0)/Al_2O_3(1\bar{1}02)$ SAW resonators oriented parallel (blue circles) and perpendicular (red squares) to the primary substrate flat and reference $Al_{0.77}Sc_{0.23}N(0001)/Al_2O_3(0001)$ SAW resonators (black triangles). The lines are a guide to the eye.

The authors thank the members of the technology department for their assistance with the device fabrication and members of the epitaxy department for their assistance with the material characterization. This work was supported by the FhG Internal Program under Grant No. Attract 005-600636. In addition, this work was partially supported by the COMET K1 center ASSIC (Austrian Smart Systems Integration Research Center).

## REFERENCES

[1] M. Akiyama, T. Kamohara, K. Kano, A. Teshigahara, Y. Takeuchi, and N. Kawahara, Adv. Mater. **21**, 593 (2009).
[2] G. Wingqvist, F. Tasnádi, A. Žukauskaitė, J. Birch, H. Arwin, L. Hultman, and F. Tasnádi, Appl. Phys. Lett. **97**, 112902 (2010).
[3] W. Wang, P. M. Mayrhofer, X. He, M. Gillinger, Z. Ye, X. Wang, A. Bittner, U. Schmid, and J. K. Luo, Appl. Phys. Lett. **105**, 133502 (2014).
[4] W. B. Wang, Y. Q. Fu, J. J. Chen, W. P. Xuan, J. K. Chen, X. Z. Wang, P. Mayrhofer, P. F. Duan, A. Bittner, U. Schmid, and J. K. Luo, J. Micromech. Microeng. **26**, 075006 (2016).
[5] G. Tang, T. Han, Q. Zhang, K. Yamazaki, T. Omori, and K. Hashimoto, in *IEEE International Ultrasonics Symposium (IUS)* (IEEE, 2016), pp. 1–4.
[6] K. Umeda, H. Kawai, A. Honda, M. Akiyama, T. Kato, and T. Fukura, in *IEEE 26th International Conference on Micro Electro Mechanical Systems (MEMS)* (IEEE, 2013), pp. 733–736.
[7] V. Pashchenko, S. Mertin, F. Parsapour, J. Li, P. Muralt, and S. Ballandras, in *Joint Conference of the European Frequency and Time Forum and IEEE International Frequency Control Symposium (EFTF/IFC)* (IEEE, 2017), pp. 565–566.
[8] A. Konno, M. Sumisaka, A. Teshigahara, K. Kano, K. Y. Hashimo, H. Hirano, M. Esashi, M. Kadota, and S. Tanaka, in IEEE International Ultrasonics Symposium (IUS) (2013), p. 1378.
[9] C.-M. Lin, Y.-J. Lai, J.-C. Hsu, Y.-Y. Chen, D. G. Senesky, and A. P. Pisano, Appl. Phys. Lett. **99**, 143501 (2011).
[10] C.-M. Lin, V. Yantchev, J. Zou, Y. Y. Chen, and A. P. Pisano, J. Microelectromech. Syst. **23**, 78 (2014).
[11] C. S. Sandu, F. Parsapour, S. Mertin, V. Pashchenko, R. Matloub, T. LaGrange, B. Heinz, and P. Muralt, Phys. Status Solidi A **216**, 1800569 (2019).
[12] C. Höglund, J. Birch, B. Alling, J. Bareño, Z. Czigány, P. O. Å. Persson, G. Wingqvist, A. Žukauskaitė, and L. Hultman, J. Appl. Phys. **107**, 123515 (2010).
[13] M. Loschonsky, D. Eisele, A. Dadgar, A. Krost, S. Ballandras, and L. Reindl, in *IEEE International Frequency Control Symposium* (IEEE, 2008), pp. 320–325.
[14] Y. Wang, J. Xu, Z. Jia, X. Xu, and Y. Xie, in *Symposium on Piezoelectricity, Acoustic Waves, and Device Applications (SPAWDA)* (IEEE, 2017), pp. 103–106.

[15]S. Tokuda, S. Takayanagi, M. Matsukawa, and T. Yanagitani, in Proceedings of IEEE International Ultrasonics Symposium, IUS (2017), pp. 2–5.
[16]N. M. Feil, N. Kurz, D. F. Urban, A. Altayara, B. Christian, A. Ding, A. Žukauskaitė, and O. Ambacher, in Proceedings of IEEE International Ultrasonics Symposium, IUS (2019), pp. 2588–2591.
[17]J. Xu, Y. Wang, Z. Jia, and Y. Xie, in *Symposium on Piezoelectricity, Acoustic Waves, and Device Applications (SPAWDA)* (IEEE, 2017), pp. 519–523.
[18]M. Suzuki, N. Sawada, and S. Kakio, Jpn. J. Appl. Phys., Part 1 **58**, SGGC08 (2019).
[19]K. Arakawa, T. Yanagitani, K. Kano, A. Teshigahara, and M. Akiyama, in Proceedings of IEEE Ultrasonics Symposium (2010), pp. 1050–1053.
[20]T. Yanagitani, K. Arakawa, K. Kano, A. Teshigahara, and M. Akiyama, in Proceedings of IEEE Ultrasonics Symposium (2010), pp. 2095–2098.
[21]M. Suzuki and T. Yanagitani, in Proceedings of Symposium on Ultrasonic Electronics (2015), p. 3P3-2.
[22]H. Yazaki, T. Soutome, R. Karasawa, S. Takayanagi, K. Yoshida, and T. Yanagitani, in Proceedings of IEEE International Ultrasonics Symposium, IUS (2018), pp. 1–4.
[23]S. Takayanagi, M. Matsukawa, and T. Yanagitani, in Proceedings of IEEE International Ultrasonics Symposium, IUS (2015), pp. 11–14.
[24]A. Kochhar, Y. Yamamoto, A. Teshigahara, K. Hashimoto, S. Tanaka, and M. Esashi, IEEE Trans. Ultrason., Ferroelectr., Freq. Control **63**, 953 (2016).
[25]M. Gomi and S. Kakio, in Proceedings of Symposium on Ultrasonic Electronics (2015), Vol. 36.
[26]Y. Lu, M. Reusch, N. Kurz, A. Ding, T. Christoph, L. Kirste, V. Lebedev, and A. Žukauskaitė, Phys. Status Solidi A **215**, 1700559 (2018).
[27]Y. Lu, M. Reusch, N. Kurz, A. Ding, T. Christoph, M. Prescher, L. Kirste, O. Ambacher, and A. Žukauskaitė, APL Mater. **6**, 076105 (2018).
[28]H.-G. Chen, S.-R. Jian, H.-L. Kao, M.-R. Chen, and G.-Z. Huang, Thin Solid Films **519**, 5090 (2011).
[29]J.-J. Wu, K. Okuura, K. Fujita, K. Okumura, H. Miyake, and K. Hiramatsu, J. Cryst. Growth **311**, 4473 (2009).
[30]J. D. Larson, P. D. Bradley, S. Wartenberg, and R. C. Ruby, in *IEEE Ultrasonics Symposium. Proceedings. An International Symposium* (IEEE, 2000), pp. 863–868.
[31]A. Ding, M. Reusch, Y. Lu, N. Kurz, R. Lozar, T. Christoph, R. Driad, O. Ambacher, and A. Žukauskaitė, in *IEEE International Ultrasonics Symposium (IUS)* (IEEE, 2018), pp. 1–9.
[32]A. H. Meitzler, H. F. Tiersten, A. W. Warner, D. Berlincourt, G. A. Coquin, and F. S. Welsh, ANSI S176-1987: *IEEE Standard on Piezoelectricity* (IEEE, New York, 1988).
[33]G. Tang, T. Han, A. Teshigahara, T. Iwaki, and K.-Y. Hashimoto, Jpn. J. Appl. Phys., Part 1 **55**, 07KD07 (2016).
[34]T. Aubert, O. Elmazria, B. Assouar, L. Bouvot, and M. Oudich, Appl. Phys. Lett. **96**, 203503 (2010).